Embolism formation and repair in vascular plants: the role of cell wall mechanics.

Wilfried Konrad and Anita Roth-Nebelsick

University of Tübingen, Germany

Abstract

The water transport system of vascular plants is permanently endangered by the formation of gas bubbles. Such embryonic gas bubbles are created by the air seeding process, i.e. the penetration of air into a vessel from adjacent, air filled vessels/tracheids or — to a much lesser extent — by spontaneous vapourization of xylem water. Because the water in xylem conduits is under tension (negative pressure), an embryonic gas bubble introduced into the water column by either source may expand into embolism, the complete disruption of the water flow inside a conduit. Embryonic gas bubbles do not necessarily evolve in this way. Instead of causing embolism they may also collapse into an — at least temporarily — stable and harmless state or even dissolute completely. If, however, embolism has occurred, a repair mechanism may start which can be expected to restore conductivity of the conduit under favourable conditions. It can be shown that the fate of bubbles appearing in a conduit under negative pressure is affected by cell wall mechanics if the conduits possess torus-margo pits. In this contribution it is examined to what extent mechanical properties of the vessel cell wall (e.g. elasticity, thickness) influence the behaviour of embryonic gas bubbles (immediate collapse vs. development towards embolism) and the processes of embolism formation. For this purpose, behaviour and possible final states of embryonic gas bubbles are calculated in terms of (a) thickness and elastic properties of the vessel cell wall, (b) xylem water pressure, (c) the initial number of air molecules within an embryonic bubble, and (d) the initial bubble radius.

Introduction

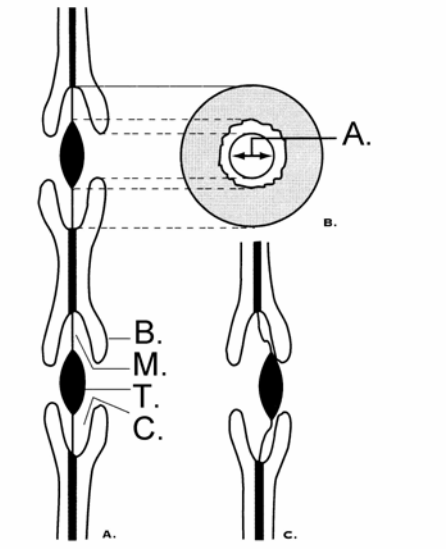

Fig. 1 (A) Two bordered pit pairs in the wall between two xylem tracheids, in side view. (B) Surface view. (C) A pressure difference — lower pressure to the right — pushes the torus against the border, thereby sealing the pit and preventing water movement.
A.:Aperture
B.: Border
M.: Pit membrane
T.: Torus
C.: Pit Cavity
(From K. Esau, Anatomy of Seed Plants*).*

Conifers possess valve-like pits (*see Fig. 1*): a pressure difference between the conduits they connect causes them to close. In this manner, an embolized conduit becomes hydraulically isolated from its

neighbours. (Also, certain angiosperms show pits with tori, such as, for example, some *Ulmus* species in their latewood (see [1]). Since it is, however, not clear whether they function in the same way as coniferous torus-margo pits, we will concentrate on coniferous wood throughout the rest of the text.) The sealing mechanism based on the torus-valve system differs from the typical angiosperm pit-membrane system since it immediately seals the embolizing conduit if a significant pressure drop develops. This rapid sealing of the tracheid has consequences for the subsequent interplay of forces acting upon the bubble and therefore on the process of embolization, because cell wall mechanics becomes significant. In this contribution, the effect of cell wall mechanics on bubble dynamics in conduits with torus-margo pits will be explored.

Physical background

After its creation by air seeding or spontaneous cavitation the development of a gas bubble is controlled by various expanding and contracting forces:

- Expanding forces: gas pressure of water vapour and air molecules and xylem water pressure (if negative)
- Contracting forces: surface force exerted by liquid/gas-interface at bubble surface and xylem water pressure (if positive)

n_a air molecules introduced into a tracheid form very rapidly a bubble of initial radius R, containing also $n_w = 4\pi R^3 p_w /(3\mathcal{R}T)$ water molecules, which vapourize almost instantaneously into the bubble (p_w: water vapour saturation pressure). Such an embryonic bubble develops further according to the following net force acting upon it (see also [2], [3])

$$F = \text{(contracting forces)} - \text{(expanding forces)} = 8\pi\gamma R + 4\pi R^2 p_s - 4\pi R^2 p_w - \frac{3\mathcal{R}T n_a}{R} \quad (1)$$

(p_s: xylem water pressure, T: temperature, $\mathcal{R}$: gas constant, γ: surface tension). The bubble radius R evolves according to the relation between the expanding and contracting forces:

$F < 0$: bubble expands
$F > 0$: bubble contracts
$F = 0$: bubble in equilibrium (stable or unstable)

An equilibrium radius R is called stable if the expanding and contracting forces react on a radial perturbation $\Delta R << R$ by restoring the bubble to the equilibrium radius R. Otherwise it is called unstable.

During gas bubble expansion, the distance between adjacent water molecules decreases because the xylem water occupies gradually less space. Macroscopically, this is equivalent to an increasing water pressure, i.e. p_s becomes less negative. The water pressure difference $p_s - p_0$ between embolizing and intact tracheids (the latter maintaining the initial water pressure p_0) induces (i) the closure of the "pit valves" (*Fig. 1*), and, (ii) a second effect: Since the tracheid walls are elastic they bulge towards the intact tracheids. Hence, the volume of the tracheids carrying the expanding bubble increases by an amount

$$\Delta V = V_0 (p_s - p_0)\, \mu \quad \text{with} \quad \mu := \frac{2 r_0}{d_0} \frac{1-\sigma^2}{E} \quad (2)$$

which is calculated from the theory of elasticity (E: Young's modulus, σ: Poisson's number, d_0: thickness of tracheid wall, r_0: radius of undeformed tracheid, L_0: tracheid length, $V_0 = \pi r_0^2 L_0$: volume of undeformed tracheid (before air seeding), p_0: tracheid water pressure before air seeding). The

difference in tracheid volume fraction occupied by (liquid) water before and after the formation of the gas bubble (and including the compressibility κ of water) affects p_s according to the following equation (see *Fig. 2*):

$$p_s = p_0 + \frac{4\,\pi\,R^3}{3\,V_0\,(\kappa+\mu)} \tag{3}$$

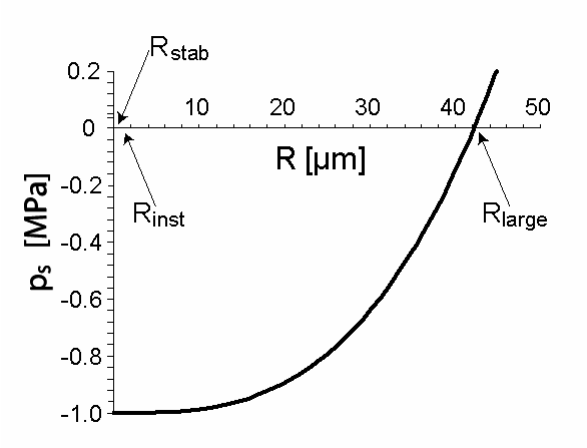

Fig. 2 Xylem water pressure p_s as function of bubble radius R as given in equation (3). R_{stab}= 0.047 µm and R_{inst} = 0.13 µm have been obtained by setting n_a = 0.5 n_{crit} in equation (5). R_{large} = 42.21 µm follows from equation (7).

Via intermolecular forces and volume change, the process of bubble expansion is thus interrelated with cell wall mechanics. In the following, it will be explored how cell wall mechanics influences bubble dynamics and therefore embolism formation. Insertion of equation (3) into (1) leads to a more general equation for the net force acting upon the gas bubble which includes the effects of cell wall properties.

$$F = \frac{16\,\pi^2}{3\,V_0\,(\kappa+\mu)}\,R^5 - 4\,\pi\,(p_w - p_0)\,R^2 + 8\,\pi\,\gamma\,R - \frac{3\,\mathcal{R}\,T\,n_a}{R} \tag{4}$$

The equilibrium radii at which a bubble ceases to expand (or shrink) are identified by setting $F = 0$ in equation (4). Closed solutions for this sixth order algebraic equation in R are not available. In the next section, approximate solutions for the interrelated system of bubble dynamics and cell wall mechanics will be presented and discussed.

Results and Discussion

Approximate solutions of equation (4) (restricted to $p_0 < p_w$) apply to either small or large bubbles

- **Small** R (necglecting first term in equation (4))

$$R_{stab} = \frac{R_{vap}}{3}\left(1 - 2\,\cos\left[\frac{1}{3}\,\arccos\left(1 - \frac{2\,n_a}{n_{crit}}\right) + \frac{\pi}{3}\right]\right)$$
$$R_{inst} = \frac{R_{vap}}{3}\left(1 + 2\,\cos\left[\frac{1}{3}\,\arccos\left(1 - \frac{2\,n_a}{n_{crit}}\right)\right]\right) \tag{5}$$

$$\text{with} \quad n_{crit} := \frac{128\,\pi\gamma^3}{81\,\mathcal{R}\,T}\frac{1}{(p_w - p_0)^2} \qquad \text{and} \qquad R_{vap} := \frac{2\,\gamma}{p_w - p_0} \tag{6}$$

- **Large** R (necglecting last two terms in equation (4))

$$R_{large} = \sqrt[3]{\frac{3}{4\,\pi}\,V_0\,(p_w - p_0)\,(\kappa + \mu)} \qquad (7)$$

R_{stab} and R_{inst} are meaningful only if the condition $n_a \leq n_{crit}$ is fulfilled. It should be noted that R_{large} is independent of n_a. Furthermore, only R_{large} (and therefore only a large nucleating bubble) depends via the quantity μ defined in equation (2) on cell wall mechanics. The equilibrium radii R_{stab} and R_{large} are stable against radial perturbations $\Delta R << R$ whereas R_{inst} is unstable. Together with (4), this implies the stability diagram of *Fig. 3* summarizing bubble behaviour: The net force F acting on a bubble is positive (i.e. contractive) in the area between the lines R_{stab}, R_{inst} and the R -axis, and beyond $R = R_{large}$. In all other (n_a,R)-areas of *Fig. 3* expression F is negative, a bubble expands towards R_{large}. For typical values of $p_0 \approx -1$MPa, stable equilibrium radii are $R_{stab} \approx 0.047$ µm and $R_{large} \approx 42.21$ µm, that is, they differ by three orders of magnitude. Thus, according to (3), if a bubble expands towards the radius R_{stab} the water pressure p_s is nearly unaffected due to its small radius, whereas the expansion of a bubble towards R_{large} causes a drastic increase of p_s (*see Fig. 2*). A small bubble at R_{stab} thus does not lead to pit valve closure since it does not cause any pressure change, neither by embolism (because it is stable) nor by affecting p_s (because it is too small). Consequently, a conduit may tolerate bubbles at stable equlibrium R_{stab} for a long time without losing its conductivity.

Bubbles, however, which expand (or shrink) towards the stable equlibrium R_{large}, induce — due to the sharp increase in p_s during their expansion — the closure of the pit. This seals the tracheid segment hydraulically from its neighbours. A residing bubble of R_{large} can only develop with a sealing torus-margo pit.

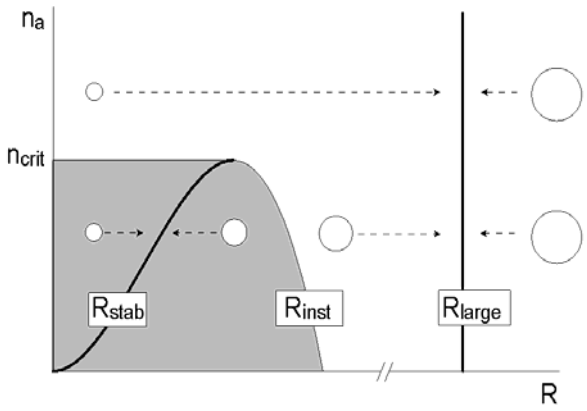

Fig. 3 Stability diagram for bubbles with initial radius R and initial air content n_a.
(i) Bubbles starting within the grey region expand or contract towards R_{stab} (solid curve, left).
(ii) Bubbles starting within other regions (white) expand or contract towards R_{large} (solid line, right).

Since R_{stab}, R_{inst} and R_{large} are solutions of $F = 0$ (equation (4)) they depend — although to a different extent — also on the parameters present in equation (4). Inspection of solutions (5) and (7) reveals the following: The positions of the lines representing R_{stab} and R_{inst} in *Fig. 3* vary only with the number n_a of air molecules injected by air seeding and with the pressure p_0 inside the tracheid before air seeding. R_{large}, however, depends also on the elastic properties of the tracheid wall, on the volume of the tracheid and on p_0: If E, d_0 or p_0 increases, R_{large} shifts to smaller values (*see Figs. 4 and 5*). If, however, r_0, L_0 or V_0 increases, R_{large} shifts to higher values (*Fig. 6*). A combination of a thicker or more rigid cell wall thus decreases the maximum radius of stable bubbles. Since smaller bubbles dissolve more readily under favourable conditions than larger bubbles, this may enhance the chances for embolism repair.

Fig. 6 shows that the connexion between R_{large} and r_0 is approximately linear for sufficiently high values of r_0. This can be understood from the structure of equations (7), (2) and the relation $V_0 = \pi\, r_0^2\, L_0$ for the tracheid volume, leading to $R_{large} \approx [3\, L_0\, (p_w - p_0)\, (1 - \sigma^2)/(2\, d_0 E)]^{(1/3)}\, r_0$. Remarkably, for typical numerical values of the quantities involved (given in *Table 1*), the value of the root is about 0.8. Hence, a bubble which has achieved stable equilibrium is “smaller” than the tracheid.

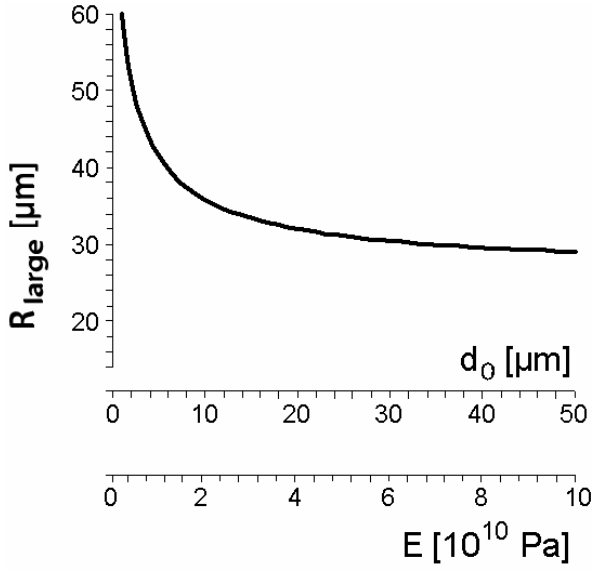

Fig. 4 Bubble radius R_{large} as function of (i) thickness d_0 of vessel wall (upper abscissa) and of (ii) Young's modulus E of the vessel wall (lower abscissa). See equations (7) and (2).

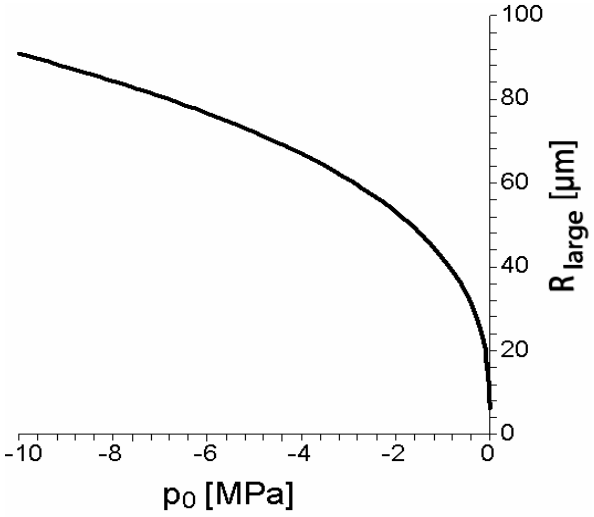

Fig. 5 Dependance of bubble radius R_{large} on initial water pressure p_0 within the vessel as given by equation (7).

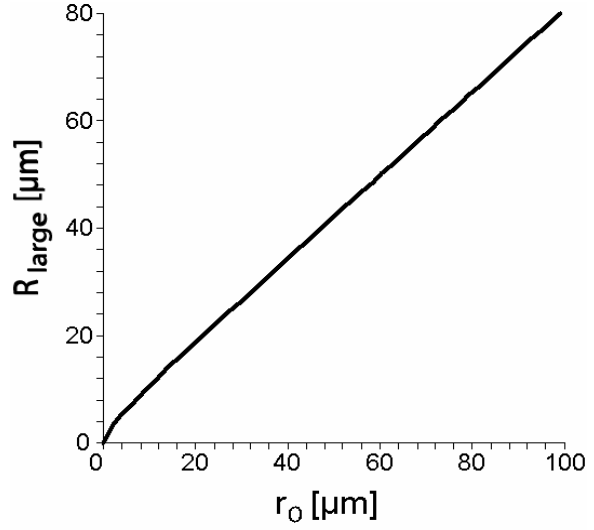

Fig. 6 Bubble radius R_{large} as function of vessel radius r_0. See equations (7), (2) and the relation $V_0 = \pi r_0^2 L_0$ for the vessel volume.

Conclusions

1. Embryonic bubbles introduced (e.g. by the air seeding process) into a tracheid possessing torus-margo pits expand (or contract) towards stable equilibrium at either bubble radius R_{stab} or R_{large}.
2. Bubbles expanding towards the radius R_{large} lead to immediate closure of the pit valves due to a pressure gradient developing between embolized and functioning tracheary element.
3. Stable bubbles with R_{large} can only form with sealing torus-margo pits.
4. R_{stab} depends only on the number n_a of air molecules injected by air seeding and on the water pressure p_0 inside the tracheid (before air seeding occured). R_{large} depends on the (elastic) properties of the tracheid wall (like Young's modulus E and wall thickness d_0) and on p_0, but not on n_a.
5. R_{large} decreases with increasing d_0, with increasing E-Modulus and with decreasing r_0. Small tracheids with thick walls may thus be favoured with respect to bubble dissolution.

Table 1 Numerical values used in the figures

Quantity	*Symbol*	*Value*
Tracheid water pressure before air seeding	p_0	-1 MPa
(Undeformed) tracheid radius	r_0	50 µm
Tracheid length	L_0	20×10^3 µm
Tracheid volume	V_0	1.57×10^8 µm^3
Thickness of tracheid wall	d_0	5 µm
Young's modulus of tracheid wall	E	10^4 MPa
Poisson's number of tracheid wall	σ	0.5
Compressibility of water	κ	5×10^{-10} Pa^{-1}

References

1. Shen, F., Gao, R., Liu, W. and Zhang, W. (2002) *Physical analysis of the process of cavitation in xylem sap.* Tree Physiology 22: 655–659.
2. Shen, F., Wenji, L., Rongfu, G., Hu, H. (2003) *A careful analysis of gas bubble dynamics in xylem*. Journal of Theoretical Biology 225: 229–233.
3. Jansen, S., Choat, B., Vinckier, S., Lens, F., Schols, P. and Smets, E. (2004): *Intervascular pit membranes with a torus in the wood of Ulmus (Ulmaceae) and related genera.* New Phytologist 163: 51-59.